Journal of Catalysis 267 (2009) 193–201

Contents lists available at ScienceDirect

Journal of Catalysis

journal homepage: www.elsevier.com/locate/jcat

Mechanistic studies and kinetics of the hydrodesulfurization of dibenzothiophene on Co–MoS_2/γ–Al_2O_3

Yinyong Sun [1], Roel Prins *

Institute of Chemical and Bioengineering, ETH Zurich, 8093 Zurich, Switzerland

ARTICLE INFO

Article history:
Received 10 June 2009
Revised 27 August 2009
Accepted 29 August 2009

Keywords:
Hydrodesulfurization
Dibenzothiophene
Hydrogenated intermediates
Mechanism
Co–MoS_2/γ–Al_2O_3
H_2S
2-Methylpiperidine

ABSTRACT

The mechanism and kinetics of the hydrodesulfurization (HDS) of dibenzothiophene (DBT) and its hydrogenated intermediates tetrahydro- and hexahydro-dibenzothiophene (THDBT and HHDBT) over Co–MoS_2/γ–Al_2O_3 were studied. The desulfurization of DBT was faster than that of THDBT and HHDBT. Cyclohexenylbenzene and cyclohexylbenzene were observed as primary products in the HDS of THDBT, indicating that THDBT was desulfurized by hydrogenolysis of the C–S bonds. Desulfurization of HHDBT occurred mainly by dehydrogenation to THDBT and subsequent desulfurization of THDBT. The addition of H_2S during HDS strongly inhibited the desulfurization of DBT and THDBT, while the addition of 2-methylpiperidine inhibited their hydrogenation. Direct desulfurization probably takes place on the metal edges of the Co–MoS_2 crystallites, while hydrogenation takes place at brim sites near the edges of the MoS_2 plane and on those Co sites that are located at the metal edge.

1. Introduction

The reduction of the sulfur content of gasoline and diesel fuel has been the subject of intensive investigations in recent years. For environmental reasons the sulfur level in many countries must be reduced to 10 ppm; for fuel cell applications the sulfur content must be below 0.1 ppm [1]. Currently, Ni–MoS_2/γ–Al_2O_3 and Co–MoS_2/γ–Al_2O_3 are widely used in industry as catalysts for the hydrodesulfurization (HDS) of sulfur-containing compounds, but to reach the required low sulfur level, more active catalysts must be developed. To design better catalysts, an in-depth understanding of the reaction mechanisms and the HDS kinetics of sulfur-containing molecules is necessary.

Dibenzothiophene (DBT) and its alkylated derivates in fuel are very difficult to desulfurize, and cause problems in deep HDS [2–6]. For that reason, DBT and its derivates are often used as model molecules in HDS studies. Several mechanistic and kinetic studies on the HDS of DBT and alkyl-substituted DBT have been carried out [2–11], but most work has focused on the parent molecules. However, to obtain sufficient kinetic data and to determine how the sulfur atoms of the hydrogenated intermediates are removed, the HDS reactions of the intermediates should be explored as well.

Recently, HDS studies of the hydrogenated intermediates of DBT and 4,6-dimethyldibenzothiophene (DMDBT) over MoS_2/γ–Al_2O_3 and Ni–MoS_2/γ–Al_2O_3 catalysts were reported [12–14] and were based on the new routes for the synthesis of large amounts of the tetrahydro (TH) and hexahydro (HH) intermediates of DBT and DMDBT [15,16]. However, studies of the HDS of hydrogenated intermediates of DBT and DMDBT have not yet been carried out over Co–MoS_2/γ–Al_2O_3 catalyst, the most common catalyst in industrial HDS. Here, we report the mechanistic and kinetic studies of the HDS of DBT and its intermediates over a Co–MoS_2/γ–Al_2O_3 catalyst. We chose DBT as a model molecule because it preferentially undergoes desulfurization by the direct desulfurization route (DDS), leading to biphenyl. Assuming that the same holds for THDBT and HHDBT, this will allow us to explain how C–S bond scission occurs.

2. Materials and methods

The Co–MoS_2/γ–Al_2O_3 catalyst (3 wt% Co and 8 wt% Mo) was prepared by incipient wetness impregnation of γ–Al_2O_3 (Condea, pore volume 0.5 cm^3/g, specific surface area 230 m^2/g). The catalyst was crushed and sieved to a 230-mesh (<0.063 mm) particle size. Further details of the catalyst preparation can be found elsewhere [17].

The reactions were carried out in continuous mode in a heated fixed-bed inconel reactor. The catalyst was sulfided in situ with 10% H_2S in H_2 (50 ml/min) at 400 °C and 1.0 MPa for 4 h. All the

* Corresponding author. Fax: +41 44 6321162.
E-mail addresses: prins@chem.ethz.ch, prins@tech.chem.ethz.ch (R. Prins).
[1] Present address: School of Chemical Engineering and Technology, Harbin Institute of Technology, Harbin 15001, China.

0021-9517/$ - see front matter © 2009 Elsevier Inc. All rights reserved.
doi:10.1016/j.jcat.2009.08.013

experiments were performed at 300 °C and 2.8 MPa H_2, because at higher temperature and H_2 pressure the conversions of the tetrahydro and hexahydro intermediates of DBT and DMDBT were too high. The gas-phase feed consisted of 1 kPa reactant (DBT, THDBT, or HHDBT), 130 kPa toluene (as solvent), 8 kPa dodecane (as GC reference), and 2.8 MPa H_2. In some experiments 35 kPa H_2S, 1 kPa 2-methylpiperidine (MPi), or 35 kPa H_2S together with 1 kPa MPi was added to the feed. From former work on the HDS of DBT, DMDBT, and their hydrogenated intermediates over MoS_2 and Ni–MoS_2 catalysts it is known that H_2S decreases the rate of the DDS reaction, while MPi decreases the rates of the DDS and HYD reactions, but decreases the HYD rate more than the DDS rate [13,14]. In this way, the separate HDS reaction routes can be better distinguished.

The reaction products were analyzed off-line, as described elsewhere [13]. Space time was defined as $\tau = w_{cat}/n_{feed}$, where w_{cat} denotes the catalyst weight and n_{feed} denotes the total molar flow to the reactor (1 g min/mol = 0.15 g h/l). The space time was changed by varying the flow rates of the liquid and the gaseous reactants, while keeping their ratio constant. Each series of experiments over a fresh catalyst started with a stabilization period of at least 15 h (overnight) at the highest space time. During two weeks of operation almost no deactivation of the catalyst was observed. A single experiment lasted 12–24 h. DBT and MPi were purchased from Acros. THDBT and HHDBT were synthesized as reported elsewhere [13].

3. Results

3.1. HDS of DBT

Fig. 1 presents the yield-time dependencies and the product selectivities measured in the HDS of DBT under different conditions. Assuming pseudo first-order kinetics, we calculated the initial rate constants k_{DBT} from the overall conversion of DBT at short space time. From these rate constants and the initial product selectivities, we calculated the initial rate constants of hydrogenation and desulfurization of DBT (k_{HYD} and k_{DDS}, respectively) (Table 1).

When H_2S and MPi were not added to the feed, the conversion of DBT reached 80% at τ = 5.2 g min/mol (Fig. 1A) and biphenyl (BP) was the main product with a constant selectivity of 95% (Fig. 1B). Because the initial rate of desulfurization of DBT (k_{DDS}) was 42 times higher than the rate of hydrogenation (k_{HYD}) (Table 1), DBT mainly desulfurizes by the DDS pathway (to BP). Small quantities of two other products, THDBT and cyclohexylbenzene (CHB), were found, and THDBT behaved as a primary product, with an initial selectivity above zero. The addition of 35 kPa H_2S led to a consid-

Table 1
Rate constants for the HDS of DBT, THDBT, and HHDBT over Co–MoS_2/γ–Al_2O_3 at 300 °C and 3.0 MPa.

Reactant	P_{H_2S} (init) kPa	P_{MPi} (init) kPa	Rate constants, mol/(g min)			
			k_{DBT}	k_{HYD}	k_{DDS}	k_{DDS}/k_{HYD}
DBT	0	0	0.43	0.01	0.42	42
	35	0	0.08	0.013	0.07	5
	0	1	0.39	0.004	0.39	98
	35	1	0.03	0.002	0.03	15
			k_{THDBT}	k_{HYD}	k_{DDS}	k_{DDS}/k_{HYD}
THDBT	0	0	0.19	0.06	0.13	2
	35	0	0.12	0.09	0.03	0.3
	0	1	0.06	0.015	0.04	2.7
	35	1	0.05	0.04	0.01	0.2
			k_{HHDBT}	k_{DEHYD}	k_{DDS}	k_{DDS}/k_{DEHYD}
HHDBT	0	0	0.83	0.7	0.1	0.1
	35	0	0.44	0.44	0	0
	0	1	0.37	0.37	0	0
	35	1	0.30	0.30	0	0

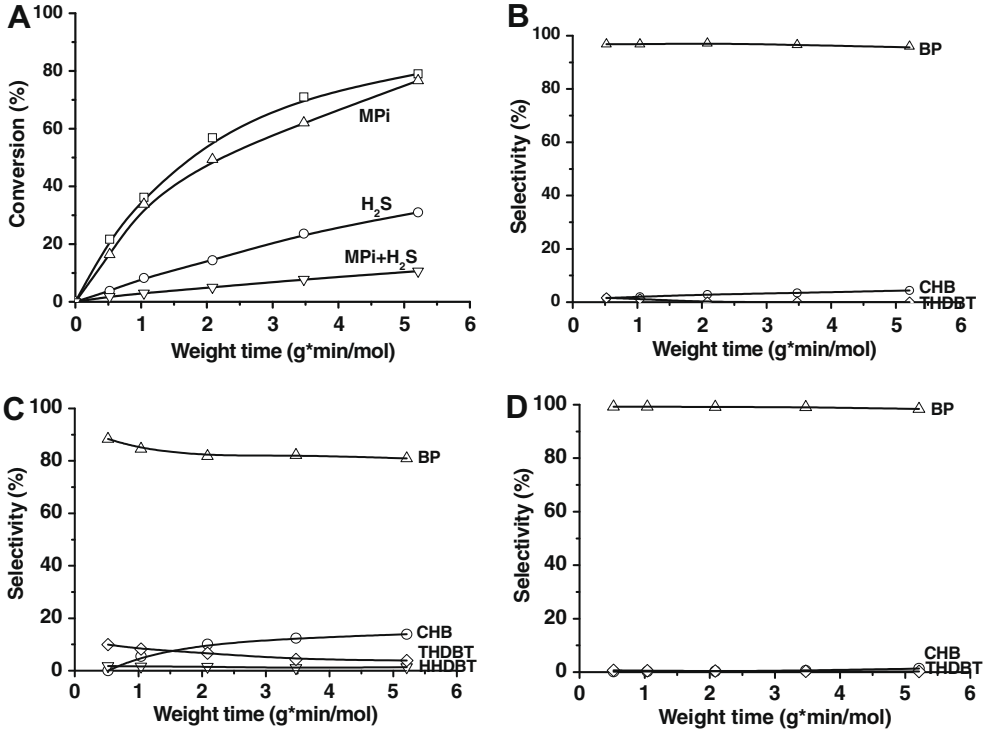

Fig. 1. HDS of DBT at 300 °C and 3.0 MPa. (A) Conversion of DBT in the absence of H_2S and MPi (□), in the presence of 35 kPa H_2S (○), in the presence of 1 kPa MPi (△), and in the presence of both 35 kPa H_2S and 1 kPa MPi (▽). Product selectivities in the absence of H_2S and MPi (B), in the presence of 35 kPa H_2S (C), and in the presence of 1 kPa MPi (D).

erable decrease in the conversion (Fig. 1A). The initial desulfurization rate k_{DDS} (of the reaction of DBT to BP) decreased by a factor six, while k_{HYD}, the rate of hydrogenation of DBT to THDBT, remained constant within the uncertainty of the measurement or even increased slightly (Table 1). But k_{DDS} was still five times higher than k_{HYD}, and DDS was the main pathway. Because of the greater relative importance of the hydrogenation route, five products were observed in the presence of H_2S (Fig. 1C): BP, THDBT, HHDBT, CHB, and a trace of bicyclohexyl (BCH). BP was the main product with a selectivity of 80%. In contrast to Ni–MoS_2/γ–Al_2O_3 [14], no promotion effect was observed for the desulfurization of DBT over Co–MoS_2/γ–Al_2O_3 when 1 kPa MPi was added. MPi slightly decreased the conversion of DBT (Fig. 1A) and the rate of desulfurization and inhibited the hydrogenation (Table 1), so that the selectivity of BP increased to 99% (Fig. 1D). The presence of both 35 kPa H_2S and 1 kPa MPi significantly inhibited the HDS process, and the conversion was only 10% at τ = 5.2 g min/mol. The results reveal that the Co–MoS_2 catalyst is much more efficient for the desulfurization of DBT than it is for the hydrogenation, and are in good agreement with the results reported in the literature [3–6,9,18–20].

3.2. HDS of THDBT

THDBT reacted rapidly in the absence of H_2S and MPi (Fig. 2A). Three products, HHDBT, CHB, and cyclohexenyl-benzene (CHEB), were observed; all three behaved as primary products, because they had selectivities above zero at τ = 0 (33, 50, and 17%, respectively, Fig. 2B). The yields of HHDBT and CHEB went through a maximum as a function of space time (Fig. 3A), demonstrating that they reacted further. At high space time (τ = 5.2 g min/mol), CHB was the main product with a selectivity of 90%, while the CHEB selectivity was 6% (Fig. 2B). This indicates that the hydrogenation of CHEB to CHB was not very fast. The k_{DDS} for THDBT was twice as high as k_{HYD} in the absence of H_2S and MPi in the feed, indicating that THDBT, too, reacted mainly by the DDS pathway over Co–MoS_2. The addition of H_2S reversed this situation, because k_{DDS} decreased by a factor four and k_{HYD} increased by 50%. As a consequence, k_{DDS}/k_{HYD} was only 0.3 in the presence of H_2S (Table 1).

The reaction of THDBT was slowed down by H_2S (Fig. 2A), and, initially, HHDBT was the main product with a selectivity of 75% at τ = 0 (Fig. 2C). The yield of HHDBT went through a maximum, while the yields of CHEB and CHB increased continuously (Fig. 3B). The decrease in the THDBT conversion (Fig. 2A) was due to a decrease in the rate of desulfurization k_{DDS} (by a factor four), while the rate of hydrogenation of THDBT to HHDBT (k_{HYD}) seemed to increase (Table 1). The addition of 1 kPa MPi inhibited the reaction of THDBT (Fig. 2A) and both k_{HYD}, the rate of initial formation of HHDBT, and k_{DDS}, the rate of initial formation of CHEB plus CHB, decreased by a factor of about four (Table 1). Apparently also the further reactions of HHDBT and CHEB were slowed down by MPi, because both HHDBT and CHEB increased continuously with space time and did not reach a maximum up to τ = 5.2 g.min/mol (Fig. 3C). The CHEB selectivity remained more or less constant at 20% from τ = 0 to 5.2 g min/mol (Fig. 2D). The addition of both MPi and H_2S strongly inhibited the desulfurization of THDBT (by a factor of thirteen) and slightly decreased the rate of hydrogenation (Table 1). Neither DBT nor BCH was observed during the HDS of THDBT indicating that the dehydrogenation of THDBT to DBT and the hydrogenation of CHB to BCH were slow under our HDS conditions.

3.3. HDS of HHDBT

When neither H_2S nor MPi was added to the feed, HHDBT reacted very fast (Fig. 4A). Until τ = 1.3 g min/mol THDBT was the main product, but thereafter CHB became the main product (Fig. 5A). The THDBT selectivity decreased and the CHB selectivity

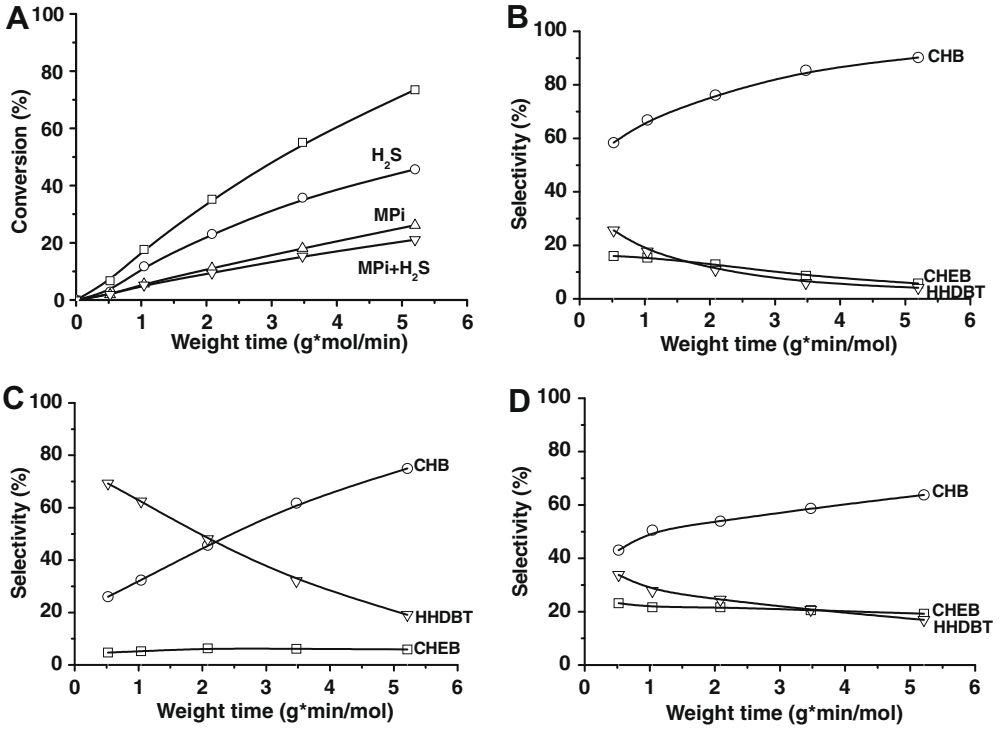

Fig. 2. HDS of THDBT at 300 °C and 3.0 MPa. (A) Conversion of THDBT in the absence of H_2S and MPi (□), in the presence of 35 kPa H_2S (○), in the presence of 1 kPa MPi (△), and in the presence of both 35 kPa H_2S and 1 kPa MPi (▽). Product selectivities in the absence of H_2S and MPi (B), in the presence of 35 kPa H_2S (C), and in the presence of 1 kPa MPi (D).

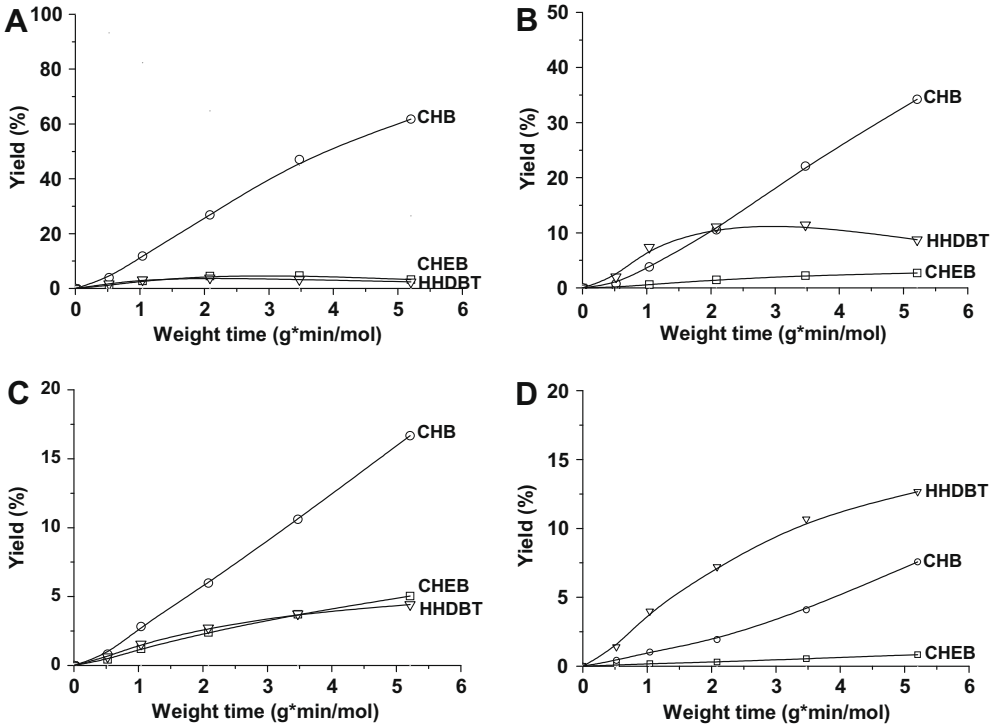

Fig. 3. HDS of 1 kPa THDBT at 300 °C and 3.0 MPa. (A) Yield of products in the absence of H_2S and MPi, (B) in the presence of 35 kPa H_2S, (C) in the presence of 1 kPa MPi, and (D) in the presence of 35 kPa H_2S and 1 kPa MPi.

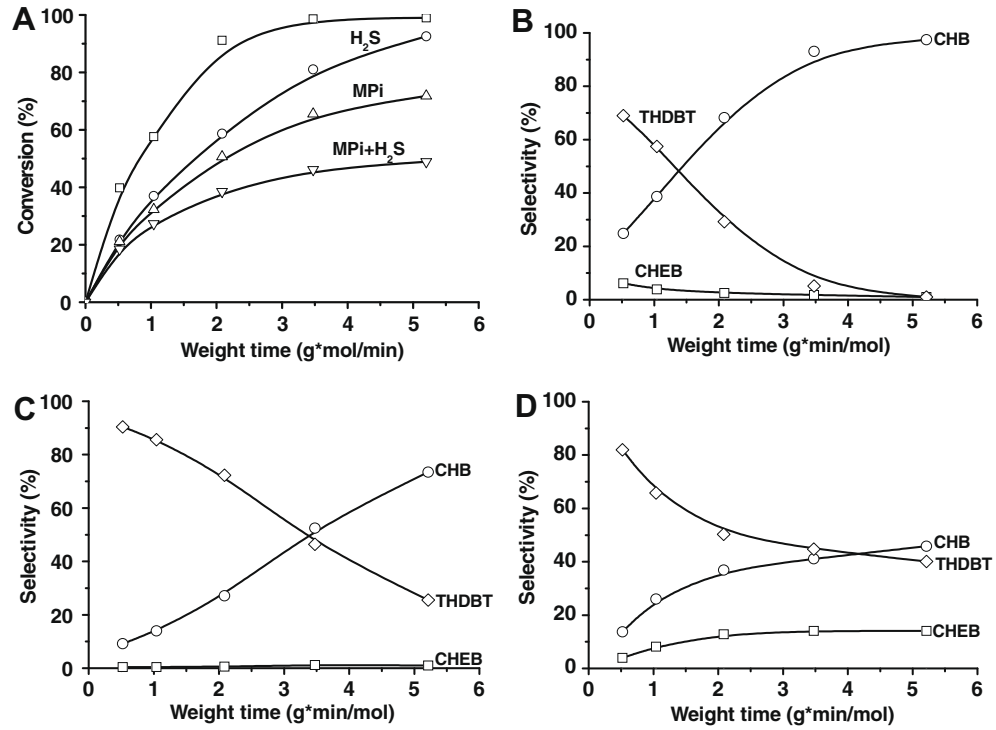

Fig. 4. HDS of HHDBT at 300 °C and 3.0 MPa. (A) Conversion of HHDBT in the absence of H_2S and MPi MPi (□), in the presence of 35 kPa H_2S (○), in the presence of 1 kPa MPi (△), and in the presence of both 35 kPa H_2S and 1 kPa MPi (▽). Product selectivities in the absence of H_2S and MPi (B), in the presence of 35 kPa H_2S (C), and in the presence of 1 kPa MPi (D).

increased with increasing space time; at τ = 5.2 g min/mol the CHB selectivity approached 100% (Fig. 4B). CHEB was also observed and its selectivity decreased with space time. The yield-time curves of THDBT and CHB indicate that THDBT reacts to CHB, because the maximum in the THDBT yield corresponds to the inflection point in the yield of CHB (Fig. 5A).

In the presence of 35 kPa H_2S, the reaction of HHDBT was inhibited (Fig. 4A). The inhibition was relatively stronger for the

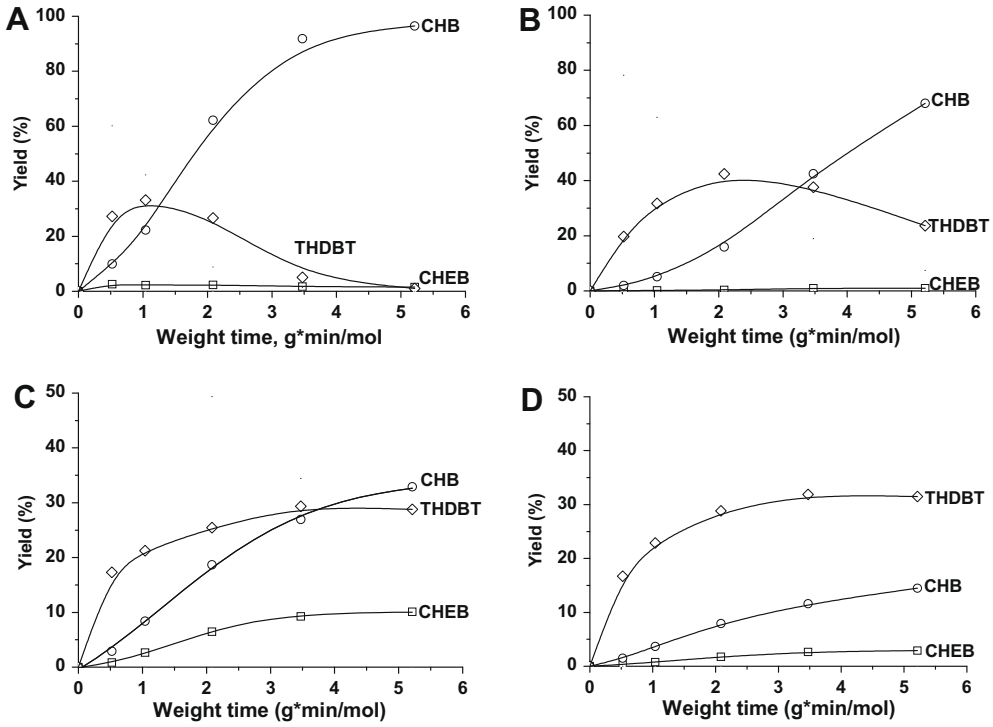

Fig. 5. HDS of 1 kPa HHDBT at 300 °C and 3.0 MPa. (A) Yield of products in the absence of H_2S and MPi, (B) in the presence of 35 kPa H_2S, (C) in the presence of 1 kPa MPi, and (D) in the presence of 35 kPa H_2S and 1 kPa MPi.

desulfurization of HHDBT than for the dehydrogenation of HHDBT to THDBT (Table 1), and, as a consequence, the initial THDBT selectivity increased (Fig. 4C). Depending on how one extrapolates the THDBT selectivity when τ goes to zero, a value between 95 and 100% is obtained (Fig. 4C). The very high initial selectivity of THDBT (Fig. 4C) and the yield-time curves of THDBT and CHB (Fig. 5B) indicate that HHDBT mainly reacts by dehydrogenation to THDBT and by subsequent desulfurization to CHB. MPi decreased the conversion of HHDBT and the further addition of H_2S decreased it even more (Fig. 4A). In both cases, the initial selectivity of THDBT approached 100% and the initial selectivities of CHB and CHEB approached 0% (Fig. 4D), again suggesting that HHDBT is first dehydrogenated to THDBT and then desulfurized to CHEB and CHB.

The reaction rate constants of all reactions of DBT, THDBT, and HHDBT in the absence of H_2S and MPi are combined in Scheme 1.

4. Discussion

4.1. Reaction rate constants

The k_{DDS} of THDBT was three or two times lower than the k_{DDS} of DBT in the absence or presence of H_2S, respectively, suggesting that the desulfurization of THDBT is relatively difficult. HHDBT, on the other hand, reacted much faster than DBT and THDBT, but this is due to the high k_{DEHYD} of HHDBT. Actually, the k_{DDS} of HHDBT is lower than that of DBT and THDBT in the absence of H_2S and MPi and decreases to zero in the presence of H_2S or MPi (Table 1). The HDS of HHDBT occurs mainly by the dehydrogenation pathway and THDBT is the primary product, which subsequently desulfurizes to the secondary products CHB and CHEB. The direct desulfurization of HHDBT is more difficult than that of THDBT and DBT, and the desulfurization rate for DBT, THDBT, and HHDBT is in the order DBT ≫ THDBT > HHDBT. This is surprising, because hydrogenation weakens one of the C–S bonds in the DBT molecule and it is assumed that a weaker bond undergoes C–S bond breaking more easily. On the other hand, aryl-metal bonds are more stable than alkyl-metal bonds and this suggests that a late transition state may explain our results. Similarly, in the Heck coupling reaction, which could be considered to be the reverse of our bond breaking reaction, C–C bonds are created by the reaction of aryl and alkenyl groups but not of alkyl groups [21].

The rate constants k_{DDS} for the desulfurization of DBT, THDBT, and HHDBT are lower for Co–MoS_2 (Table 1) than the corresponding rate constants for Ni–MoS_2 [14] in the absence of H_2S and MPi

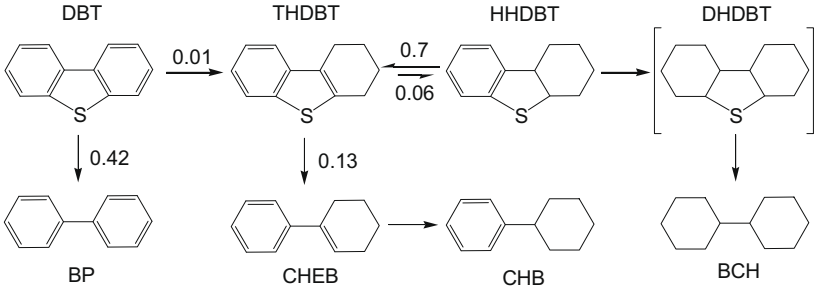

Scheme 1. Intermediates and final hydrocarbon products in the HDS of dibenzothiophene.

in the feed. Nevertheless, in industry, Co–MoS_2 is the catalyst of choice for HDS and Ni–MoS_2 is used only when strong hydrogenation is required in addition to HDS. The different selectivity and the sensitivity of Co–MoS_2 and Ni–MoS_2 to H_2S explain this. First, compared with a Ni–MoS_2 catalyst [14], the Co–MoS_2 catalyst is a relatively weaker catalyst for hydrogenation, because k_{HYD} was six times lower and k_{DDS} only 2.7 times lower for the Co–MoS_2 catalyst than for the Ni–MoS_2 catalyst. Thus, Co–MoS_2 has a higher DDS selectivity than Ni–MoS_2 and a lower H_2 consumption. Second, whereas Ni–MoS_2 is the better HDS catalyst in the absence of H_2S, with higher k_{DDS} and k_{HYD} for DBT as well as THDBT [14], in the presence of 35 kPa H_2S the rate constants k_{DDS} of DBT and THDBT are slightly higher for Co–MoS_2 than for Ni–MoS_2, while the rate constants k_{HYD} are almost equal. This might explain why, under industrial HDS conditions, Co–MoS_2 is preferred.

4.2. HDS mechanism of DBT

The breaking of a C–S bond may take place by elimination or by hydrogenolysis. If aryl C–S bond breaking were to take place by elimination, then a phenyl ring first had to be hydrogenated to create a β–H atom. For DBT, a dihydro intermediate was therefore proposed [9], but this intermediate seems unlikely, because it would lead to much higher activation energy than experimentally observed. Furthermore, the hydrogenation of the double bond requires π adsorption, which cannot explain why methyl groups in the 4- and 6-position constitute a steric problem in the DDS route of the HDS of 4,6-DMDBT. Diminished steric hindrance in the hydrogenated intermediates does not play a role in the elimination scheme of DBT, because the rate-determining step will be the addition of two H atoms to one ring of DBT. The fact that k_{DDS} decreases in the order DBT $\gg$ THDBT > HHDBT is another indication that the DDS pathway does not go through elimination. Therefore, the DDS reaction is probably an actual hydrogenolysis reaction, as originally suggested by Broderick and Gates [18], in which DBT and hydrogen atoms on the catalyst surface react directly to BP. The two aryl C–S bonds of DBT will break in two steps, first forming 2-phenyl-thiophenol and then BP. The very fast HDS reaction of thiophenol [13] explains why this intermediate has never been observed. DFT calculations by Weber and van Veen demonstrated that the hydrogenolysis reactions of the C–S bonds of DBT can occur with moderate activation energies [22]. Homogeneous catalysis studies by Jones [23], Angelici and others [24] have shown that a metal atom of an organometal complex can easily insert into the C–S bond of thiophene and DBT. Such C–M–S complexes might also be intermediates in the hydrogenolysis of C–S bonds on a metal sulfide surface.

In the HDS of THDBT, CHEB behaved as a primary product (with increasing selectivity at decreasing space time), while CHB behaved as a primary as well as a secondary product, because it had a non-zero selectivity at $\tau = 0$, as it would if it were a primary product, but its selectivity decreased with decreasing space time, as it would if it were a secondary product (Fig. 2). CHEB may form by hydrogenolysis of the aryl C–S bond of THDBT (to form 2-phenyl-cyclohexene-1-thiol) or of the vinyl C–S bond (to form 2-(cyclohexen-1-yl)-thiophenol) (Scheme 2). Breaking of the second C–S bond then leads to CHEB. It is also possible that the first hydrogenation takes place to 2-phenyl-cyclohexanethiol or 2-cyclohexyl-thiophenol, which then hydrogenolyzes to CHB. The secondary reaction, with CHEB as the intermediate, explains why the CHEB selectivity decreases and the CHB selectivity increases with increasing space time (Fig. 2).

When HHDBT was the reactant, CHEB and CHB generally behaved as secondary products (Fig. 4C and D). Only in the absence of H_2S and MPi did CHEB behave as a primary product (Fig. 4B). This indicates that HHDBT reacts mainly to THDBT and that CHEB and CHB form by the fast reaction of HHDBT to THDBT and then to CHEB and CHB. The formation of CHEB from HHDBT, when no H_2S and MPi were added to the feed, suggests that this occurred by elimination. When the cycloalkyl C–S bond of HHDBT is broken first, 2-cyclohexyl-thiophenol forms by hydrogenolysis and 2-cyclohexen-1-yl-thiophenol by elimination (Scheme 3). The aryl C–S bond can only be broken by hydrogenolysis, which results in the formation of 2-phenyl-cyclohexanethiol. Cristol et al. carried out a DFT calculation of the desulfurization of dihydrobenzothiophene over the metal and sulfur edges of MoS_2. It showed that there is no thermodynamical difference between the hydrogenolysis of the aryl and alkyl C–S bonds in dihydrobenzothiophene [25], while the DFT calculation of Yao et al. with a Mo_3S_9 cluster showed that the hydrogenolysis of the aryl C–S bond in dihydrobenzothiophene has slightly lower activation energy than the breaking of the alkyl C–S bond [26]. Because of the similarity of HHDBT to dihydrobenzothiophene, with one part of the molecule being aromatic and the other part being aliphatic, some of the desulfuriza-

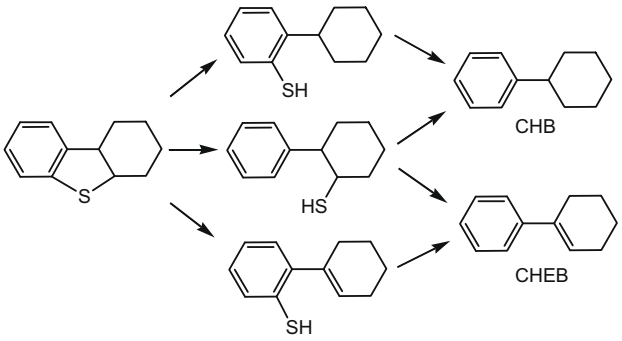

Scheme 3. Proposed reactions of HHDBT–CHEB and CHB.

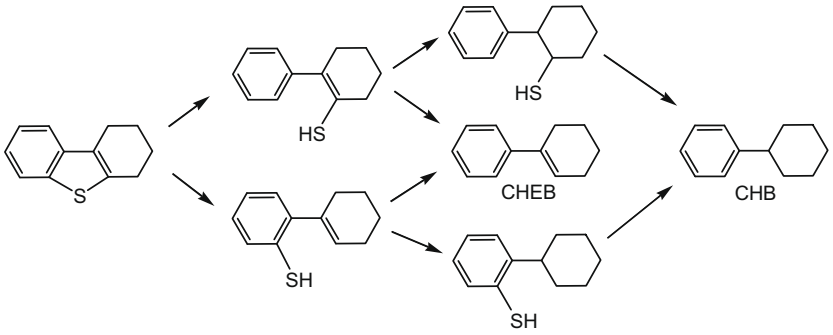

Scheme 2. Proposed reactions of THDBT to CHEB and CHB.

tion of HHDBT may well take place by hydrogenolysis of the aryl C–S bond, followed by elimination of H_2S from the resulting 2-phenyl-cyclohexanethiol to form CHEB or by hydrogenolysis to form CHB (Scheme 3).

4.3. Catalytic sites

Fig. 6 shows a comparison of the DDS and HYD rate constants for the reactions of DBT and THDBT and the DDS and DEHYD rate constants for HHDBT obtained for Co–MoS_2 in the absence and presence of H_2S (present results) with the rate constants obtained for Ni–MoS_2 [14] and MoS_2 [13]. Over Co–MoS_2 and Ni–MoS_2, the reaction took place at 3 MPa and over MoS_2 at 5 MPa, because at 3 MPa the rates over MoS_2 were low. Therefore, when comparing the data one should bear in mind that the rate constants for MoS_2 are overestimated. The results show some clear trends. First, H_2S decreases all DDS rate constants, whereas it hardly influences the HYD rate constants in all cases but two (DBT over Ni–MoS_2 and HHDBT over Co–MoS_2). The effect of H_2S on the DDS and HYD rate constants for DBT was reported before [9,18–20,27]. Second, the DDS rate constants for all three molecules decrease in the order Ni–MoS_2 > Co–MoS_2 > MoS_2, while the HYD rate constants of all three catalysts for a given molecule and under given conditions (presence or absence of H_2S) are more or less the same within the uncertainty of the measurements. Only in the case of DBT, in the absence of H_2S, was the HYD rate constant for Ni–MoS_2 higher than those for Co–MoS_2 and MoS_2. Third, the DDS rate constants decrease in the order DBT > THDBT > HHDBT for Ni–MoS_2 and Co–MoS_2 but in the order DBT < THDBT ≈ HHDBT for MoS_2. As indicated in Section 4.1, the reason for the former order may be that aryl-metal bonds are more stable than alkyl-metal bonds. It is unclear why the order is different for MoS_2. Fourth, the HYD rate constant for THDBT is higher than that for DBT for all three catalysts. This must be due to the easier hydrogenation of an olefin (THDBT) than of a phenyl ring (DBT).

The strong dependence of the DDS reactions on the H_2S pressure means that the DDS of all three molecules takes place at a metal atom on the surface of the metal sulfide with a free

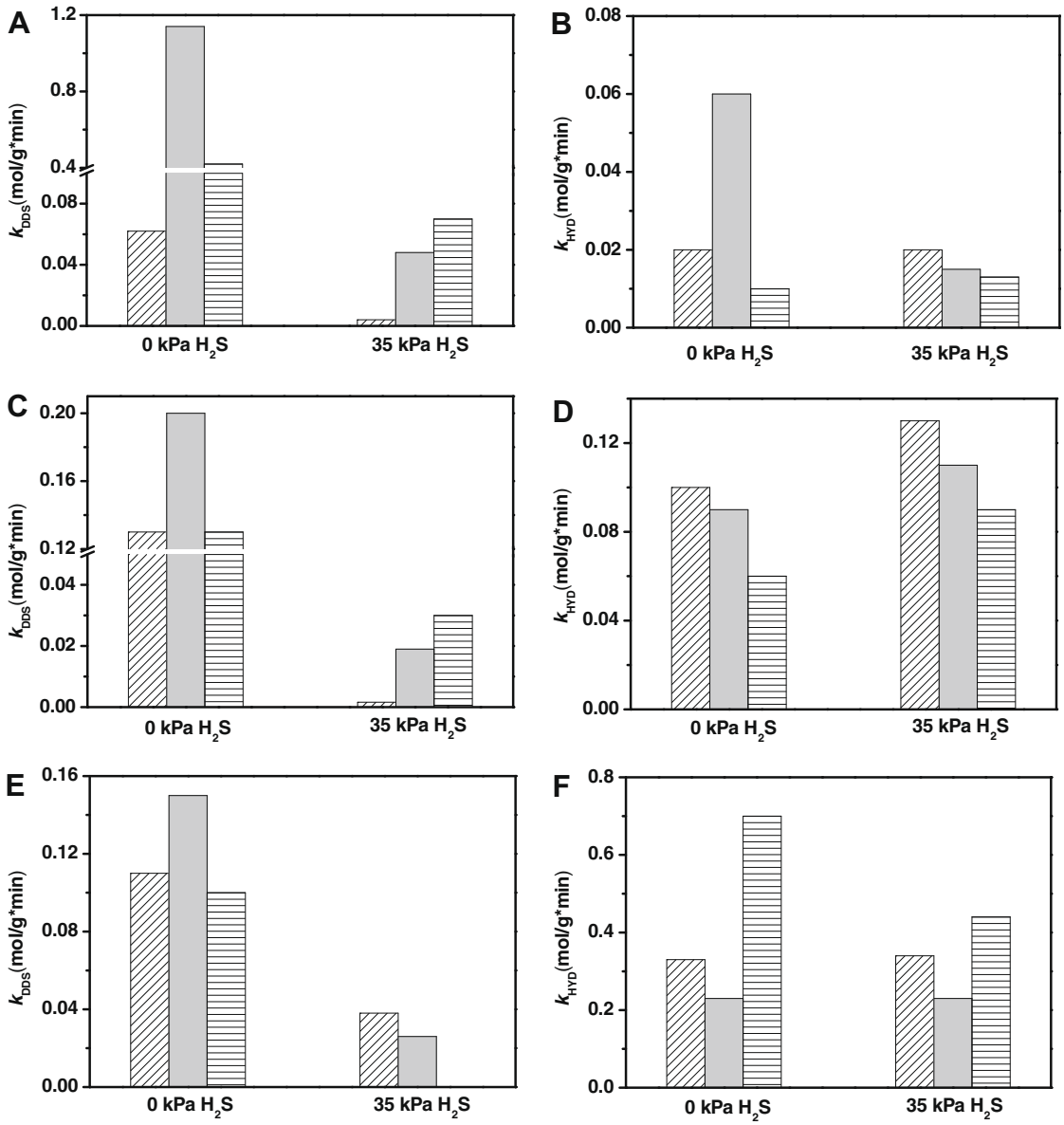

Fig. 6. Comparison of DDS and HYD or DEHYD rate constants over MoS_2 (▨), Ni–MoS_2 (▭), and Co–MoS_2 (▭) catalysts in the presence of 0 and 35 kPa H_2S partial pressure for the HDS reactions of DBT ((A) and (B)), THDBT ((C) and (D)), and HHDBT {(E) and (F)}. The data of the reactions over Co–MoS_2 and Ni–MoS_2 catalysts were obtained at 3 MPa and those over MoS_2 at 5 MPa, because at 3 MPa the rates over MoS_2 were low.

coordination position, so that competition between the sulfur-containing molecule and H_2S for adsorption can take place. The rate-determining step in the DDS over MoS_2, Co–MoS_2, and Ni–MoS_2 cannot be the removal of the S atom from the catalytic site by H_2S desorption, following the reaction of the sulfur-containing molecule on the site, as proposed by Neurock and van Santen [28]. Otherwise the HDS of all the sulfur-containing molecules would be equally fast and zero order. One explanation for the increase in k_{DDS} in the order MoS_2 < Co–MoS_2 < Ni–MoS_2 may be that the Co and Ni promoters increase the number of free coordination positions on the MoS_2 surface and that the Mo atoms, with the free coordination position, act as DDS sites. However, this is in contrast to the different activation energy and reaction order in the HDS of thiophene for MoS_2, Co–MoS_2 [29], and Ni–MoS_2 [30] and to the inhibiting effect of H_2S in the HDS of DBT, THDBT, and HHDBT, which is different for Co–MoS_2 (present results) compared to MoS_2 [13] and Ni–MoS_2 [14]. A second possibility may be that mixed Co–Mo or Ni–Mo sites are responsible for the desulfurization, as DFT calculations have shown that S atoms, situated between a Mo and a Co or Ni promoter atom in Co–MoS_2 and Ni–MoS_2, are less strongly bonded than S atoms at the edges of MoS_2 [31–33]. As a consequence, S atoms in the bridge position between a Mo and a Co or Ni atom can be removed more easily and Mo atoms adjacent to Co and Ni atoms at the surface of Co–MoS_2, respectively, Ni–MoS_2 have at least one free coordination position. A third model proposed that the Co and Ni atoms themselves are the active sites in the promoted catalysts [34]. In that case the order Ni–MoS_2 > Co–MoS_2 > MoS_2 for the DDS rate constants depends on the number of free coordination positions and the intrinsic rate of the M site.

DFT studies have indicated that Co and Ni promoter atoms may be located at both edges of MoS_2 particles, but that the most stable position for Co atoms is on the sulfur edges, while Ni atoms prefer the metal edges [31–33]. The most stable coordination for Mo on the sulfur edges and those Co and Ni atoms that are located on the sulfur edges of Co–MoS_2 and Ni–MoS_2, respectively, is a tetrahedral coordination by four S atoms [32]. Experimental STM studies by Lauritsen et al. have shown that MoS_2 particles that are prepared on a gold surface and decorated with Co or Ni atoms have the Co atoms at the sulfur edge with tetrahedral sulfur coordination, while the Ni atoms are present at both edges [35]. Because the maximum coordination number of transition-metal atoms is usually six, the Mo, Co, and Ni atoms have the geometrical possibility to adsorb a sulfur-containing molecule in σ fashion. The alternative, to create a vacancy by removal of a sulfur atom, leaves a metal atom with only three sulfur ligands and, thus, requires high energy.

The number of free coordination positions at the metal edges of MoS_2 and Co–MoS_2 and Ni–MoS_2 is different for the Mo, Co, and Ni atoms. DFT calculations predict that six sulfur atoms trigonal prismatically coordinate the Mo atoms on the metal edges of MoS_2 and that these sulfur atoms are strongly bonded [32,33]. One DFT calculation predicts very few S vacancies, if any at all [36], while another DFT calculation predicts that, under HDS conditions ($H_2S/H_2 \approx 0.01$), about 20% of the Mo atoms on the metal edges may have a sulfur vacancy [37]. On the other hand, the Co and Ni atoms on the metal edges of Co–MoS_2 and Ni–MoS_2, respectively, have square-planar sulfur coordination [32] and, thus, have a free coordination position to adsorb a sulfur-containing molecule in σ fashion. DFT calculations have shown that such Ni atoms adsorb H_2S quite strongly [37]. Co atoms in the square-planar configuration usually bind an additional fifth ligand strongly, and this might explain why Ni–MoS_2 has a higher activity than Co–MoS_2 for DBT, THDDBT, and HHDBT and why the reaction order for thiophene during HDS is lower for Co–MoS_2 [29] than for Ni–MoS_2 [30]. Taken from the perspective of free coordination positions for the adsorption of sulfur-containing molecules, DDS reactions may thus take place on the sulfur edges of MoS_2, Co–MoS_2, and Ni–MoS_2, on the metal edges of Co–MoS_2 and Ni–MoS_2, and perhaps on the metal edges of MoS_2. The increasing inhibition by H_2S in the order MoS_2 < Co–MoS_2 < Ni–MoS_2 suggests that the contribution of the DDS reactions that take place on the metal edges increases in the same order.

The HYD rate constants are hardly influenced by H_2S, with the exception of the HYD rate constant for DBT over Ni–MoS_2, which clearly decreases in the presence of H_2S (Fig. 6). This indicates that the corresponding rate-determining HYD steps do not take place on a site with a free coordination position or sulfur vacancy. STM investigations have shown that the so-called brim sites, on the basal planes of MoS_2 right behind the edges, have a metallic character [35,38]. Hydrogenation of sulfur-containing aromatic molecules can then take place on the brim sites [39]. Since the basal planes are fully sulfided, H_2S does not affect the hydrogenation over the MoS_2-based catalysts. Adsorption on brim sites, in π fashion on the basal plane of MoS_2, right behind the edge, would, geometrically, not constitute a problem. If, on the other hand, hydrogenation were to take place on the edges, then π adsorption on metal atoms on the sulfur edge would not be feasible, while π adsorption on metal atoms on the metal edge would be possible only if at least two neighboring free coordination positions were present [25]. This is inconceivable for MoS_2 [36,37] but possible for Ni–MoS_2, because all Ni atoms at the metal edge of Ni–MoS_2 (with a coverage of 100% Ni) have a free coordination position [32]. Co atoms are preferentially located at the S edges; if located on the metal edge they tend to occupy only 50% of the positions at the metal edge. These Co atoms have neighboring Mo atoms, which are topped by a sulfur atom [33,37], and there are few neighboring sites with two free coordination positions. This suggests that hydrogenation over Ni–MoS_2 may take place not only at brim sites near the edges of the MoS_2 plane, but also at Ni sites at the metal edge. This would explain why only in the case of Ni–MoS_2 does the DDS rate constant for DBT decrease with increasing H_2S pressure (Fig. 6), because H_2S adsorbs strongly on the Ni atoms [37].

5. Conclusions

The hydrodesulfurization of DBT, THDBT, and HHDBT on Co–MoS_2/γ–Al_2O_3 was studied in the absence and presence of H_2S and MPi, and the rate constants of all the reaction steps were obtained. The Co–MoS_2/γ–Al_2O_3 catalyst was relatively efficient for desulfurization but relatively weak for hydrogenation. The desulfurization of DBT was faster than that of THDBT and HHDBT. Desulfurization of THDBT occurred directly to CHEB and CHB, but desulfurization of HHDBT occurred mainly by dehydrogenation to THDBT and subsequent desulfurization of THDBT. In most cases C–S bond breaking occurred by hydrogenolysis. Direct desulfurization probably takes place on the metal edges, while hydrogenation takes place at brim sites near the edges of the MoS_2 plane and on Co and Ni sites at the metal edge.

References

[1] R.T. Yang, A.J. Hernández-Maldonado, F.H. Yang, Science 301 (2003) 79.
[2] M. Houalla, N.K. Nag, A.V. Sapre, D.H. Broderick, B.C. Gates, AIChE J. 24 (1978) 1015.
[3] M.J. Girgis, B.C. Gates, Ind. Eng. Chem. Res. 30 (1991) 2021.
[4] H. Topsøe, B.S. Clausen, F.E. Massoth, Hydrotreating Catalysis, Science and Technology, Springer, Berlin, 1996.
[5] D.D. Whitehurst, T. Isoda, I. Mochida, Adv. Catal. 42 (1998) 345.
[6] R. Prins, in: G. Ertl, H. Knözinger, F. Schüth, J. Weitkamp (Eds.), Handbook of Heterogeneous Catalysis, vol. 6, second ed., Wiley-VCH, Weinheim, 2008, p. 2695.
[7] A. Röthlisberger, R. Prins, J. Catal. 235 (2005) 229.
[8] T. Kabe, A. Ishihara, Q. Zhang, Appl. Catal. A 97 (1993) L1.

[9] F. Bataille, J.L. Lemberton, P. Michaud, G. Pérot, M.L. Vrinat, M. Lemaire, E. Schulz, M. Breysse, S. Kasztelan, J. Catal. 191 (2000) 409.
[10] M. Macaud, A. Milenkovic, E. Schulz, M. Lemaire, M. Vrinat, J. Catal. 193 (2000) 255.
[11] M. Egorova, R. Prins, J. Catal. 225 (2004) 417.
[12] X. Li, A. Wang, M. Egorova, R. Prins, J. Catal. 250 (2007) 283.
[13] H. Wang, R. Prins, J. Catal. 258 (2008) 153.
[14] H. Wang, R. Prins, J. Catal. 264 (2009) 31.
[15] P. Kukula, V. Gramlich, R. Prins, Helv. Chim. Acta 89 (2006) 1623.
[16] Y. Sun, H. Wang, R. Prins, Tetrahedron Letters 49 (2008) 2063.
[17] M. Egorova, R. Prins, J. Catal. 241 (2006) 162.
[18] D.H. Broderick, B.C. Gates, AIChE J. 27 (1981) 663.
[19] M.L. Vrinat, L. de Mourgues, J. Chim. Phys. 79 (1982) 45.
[20] Q. Zhang, W. Qian, A. Ishihara, T. Kabe, Sekiyu Gakkaishi 40 (1997) 185.
[21] P.W.N.M. van Leeuwen, Homogeneous Catalysis, Kluwer, Dordrecht, 2004.
[22] Th. Weber, J.A.R. van Veen, Catal. Today 130 (2008) 170.
[23] T.A. Atesin, W.D. Jones, Organometallics 27 (2008) 53.
[24] R.J. Angelici, in: Th. Weber, R. Prins, R.A. van Santen (Eds.), Transition Metal Sulphides. Chemistry and Catalysis, Kluwer, Dordrecht, 1998, p. 89.
[25] S. Cristol, J.F. Paul, E. Payen, D. Bougeard, J. Hafner, F. Hutschka, Stud. Surf. Sci. Catal. 128 (1999) 327.
[26] X.Q. Yao, Y.W. Li, H. Jiao, J. Mol. Struct. Theochem 726 (2005) 67.
[27] T. Kabe, Y. Aoyama, D. Wang, A. Ishihara, W. Qian, M. Hosoya, Q. Zhang, Appl. Catal. A 209 (2001) 237.
[28] M. Neurock, R.A. van Santen, J. Am. Chem. Soc. 116 (1994) 4427.
[29] E.J.M. Hensen, H.J.A. Brans, G.M.H.J. Lardinois, V.H.J. de Beer, J.A.R. van Veen, R.A. van Santen, J. Catal. 192 (2000) 98.
[30] A. Borgna, E.J.M. Hensen, J.A.R. van Veen, J.W. Niemantsverdriet, J. Catal. 221 (2004) 541.
[31] L.S. Byskov, J.K. Nørskov, B.S. Clausen, H. Topsøe, J. Catal. 187 (1999) 109.
[32] E. Krebs, B. Silvi, P. Raybaud, Catal. Today 130 (2008) 160.
[33] P. Raybaud, J. Hafner, G. Kresse, S. Kasztelan, H. Toulhoat, J. Catal. 190 (2000) 128.
[34] J.C. Duchet, E.M. van Oers, V.H.J. de Beer, R. Prins, J. Catal. 80 (1983) 386.
[35] J.V. Lauritsen, J. Kibsgaard, G.H. Olesen, P.G. Moses, B. Hinnemann, S. Helveg, J.K. Nørskov, B.S. Clausen, H. Topsøe, E. Lægsgaard, F. Besenbacher, J. Catal. 249 (2007) 220.
[36] J.F. Paul, E. Payen, J. Phys. Chem. B 107 (2003) 4057.
[37] M. Sun, J. Adjaye, A.E. Nelson, Catal. Today 105 (2005) 36.
[38] J.V. Lauritsen, S. Helveg, E. Laegsgaard, I. Stensgaard, B.S. Clausen, H. Topsøe, F. Besenbacher, J. Catal. 197 (2001) 1.
[39] P.G. Moses, B. Hinnemann, H. Topsøe, J.K. Nørskov, J. Catal. 248 (2007) 188.